



Natural convective flow between isothermal concentric spheres  
by Shiu-hau Yin

A dissertation submitted to the Graduate Faculty in partial fulfillment of the requirements for the degree of DOCTOR OF PHILOSOPHY in Aerospace and Mechanical Engineering  
Montana State University  
© Copyright by Shiu-hau Yin (1972)

**Abstract:**

Natural convective flow of air and water between isothermal concentric spheres was experimentally investigated. Different visualization techniques were utilized for each specified fluid. A special visualization technique was developed for water as the working medium in this study. The visualization of the flow pattern was accomplished by introducing a well mixed and prepared solution of distilled water containing a very minute amount of liquid "Ajax" detergent into the annulus and transversely illuminating vertical diameter.

For air in the gap, smoke was introduced. A qualitative description of the flow patterns obtained for each spherical combination studied is presented, and these descriptions are supplemented by photographs of the flow. Motion pictures of each distinctive type of flow pattern found to occur in this investigation were also obtained.

For air as the working fluid, distinct steady and unsteady patterns were obtained for various diameter ratios ranging from 1.40 to 2.17 and for Grashof numbers (based on gap thickness) ranging from  $7.0 \times 10^3$  to  $1.2 \times 10^6$ . The flow patterns at the lower Grashof numbers qualitatively agree with those obtained in previous studies. The inception of instabilities characterized by periodic interior contractions or three-dimensional spiral flow in the spherical annuli was compared to the case of horizontal cylindrical annuli.

For water as working fluid, the most common basic flow pattern, the steady dog-face type, occurred in the three largest diameter ratios investigated. This kind of flow pattern has never been observed before, but it does correlate quite well with the temperature profiles obtained in the heat transfer study. A formation of tertiary flow in the weak shear layer between two secondary cells occurred for the diameter ratio of 1.78 ( $L/D_i=0.39$ ) at high Grashof numbers. As the Grashof number was increased above certain transition points, an unsteady dog—face type flow, or a three-dimensional spiral flow, was observed. In this study, the diameter ratio ranged from 1.09 to 2.17 and the Grashof number based on gap thickness ranged from  $1.7 \times 10^3$  to  $1.4 \times 10^7$ .

A tabular form of the experimental results for each test fluid is presented to provide categorization of the fluid-flow behavior within the available ranges of independent variables.

NATURAL CONVECTIVE FLOW BETWEEN  
ISOTHERMAL CONCENTRIC SPHERES

by

SHIU-HAU YIN

A dissertation submitted to the Graduate Faculty  
in partial fulfillment of the requirements for the degree

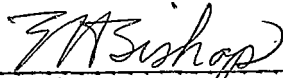
of

DOCTOR OF PHILOSOPHY

in

Aerospace and Mechanical Engineering

Approved:



Head, Major Department



Chairman, Examining Committee



Graduate Dean

MONTANA STATE UNIVERSITY  
Bozeman, Montana

March, 1972

## ACKNOWLEDGEMENT

The author wishes to express his sincere thanks and appreciation to all those who have aided in this work. Special thanks are due to Dr. J. A. Scanlan, Dr. E. H. Bishop, and Dr. R. E. Powe for their advice, guidance, and encouragement. Thanks also go to Mr. Gordon Williamson for his assistance in constructing the entire apparatus. The writer is especially appreciative of the patience and understanding of his wife, Sandra.

The work reported in this thesis was supported by the Atomic Energy Commission under Contract Number AT(45-1)-2214.

## TABLE OF CONTENTS

Chapter	Page
VITA . . . . .	ii
ACKNOWLEDGEMENT . . . . .	iii
LIST OF TABLES . . . . .	v
LIST OF FIGURES . . . . .	vi
ABSTRACT . . . . .	x
NOMENCLATURE . . . . .	xi
I. INTRODUCTION . . . . .	1
II. LITERATURE REVIEW . . . . .	4
III. EXPERIMENTAL SYSTEM . . . . .	17
APPARATUS . . . . .	17
PROCEDURE . . . . .	34
IV. EXPERIMENTAL RESULTS AND DISCUSSION . . . . .	39
FLOW PATTERN DESCRIPTIONS . . . . .	41
SUMMARY OF EXPERIMENTAL RESULTS . . . . .	86
DISCUSSION OF RESULTS . . . . .	94
V. CONCLUSIONS AND RECOMMENDATIONS . . . . .	103
APPENDIX I. GOVERNING DIFFERENTIAL EQUATIONS . . . . .	107
APPENDIX II. EQUIPMENT LIST . . . . .	112
APPENDIX III. COMPUTER PROGRAMS . . . . .	115
BIBLIOGRAPHY . . . . .	126

## LIST OF TABLES

Table	Page
1. Gap Working Fluid and Associated Geometric Combinations . . . . .	38
2. Summary of Results for Air as the Gap Working Fluid . . . .	89
3. Summary of Results for Water as the Gap Working Fluid . .	92

## LIST OF FIGURES

Figure	Page
1. Assembled Apparatus with Water Cooling System . . . . .	18
2. Schematic Diagram of Experimental System (Water as Gap Fluid) . . . . .	19
3. Schematic Diagram of Experimental System (Air as Gap Fluid) . . . . .	20
4. Interior of Inner Sphere . . . . .	22
5. Glass Hemispheres . . . . .	24
6. Installation of Inner Sphere Inside the Glass Sphere . . .	25
7. Particles in Water within the Spherical Annulus before Heating . . . . .	31
8. Steady Crescent Eddy Pattern for $D_o/D_i = 2.17$ , $L/D_i =$ $0.59$ , $N_{GR_L} = 72,000$ , $N_{RA_L} = 51,000$ . . . . .	42
9. Photograph Showing Onset of Steady Kidney-Shaped Eddy Pattern for $D_o/D_i = 2.17$ , $L/D_i = 0.59$ , $N_{GR_L} =$ $166,500$ , $N_{RA_L} = 118,000$ . . . . .	44
10. Steady Kidney-Shaped Eddy Pattern for $D_o/D_i = 2.17$ $L/D_i = 0.59$ , $N_{GR_L} = 295,800$ , $N_{RA_L} = 209,600$ . . . . .	45
11. Steady Kidney-Shaped Eddy Pattern for $D_o/D_i = 2.17$ , $L/D_i =$ $0.59$ , $N_{GR_L} = 555,000$ , $N_{RA_L} = 393,000$ . . . . .	47
12. Steady Modified Kidney-Shaped Eddy Pattern for $D_o/D_i = 2.17$ , $L/D_i = 0.59$ , $N_{GR_L} = 1,056,000$ , $N_{RA_L} = 746,000$ . . . . .	48
13. Steady Crescent Eddy Pattern for $D_o/D_i = 1.78$ , $L/D_i =$ $0.39$ , $N_{GR_L} = 93,100$ , $N_{RA_L} = 66,000$ . . . . .	50

Figure	Page
14. Steady Kidney-Shaped Eddy Pattern for $D_o/D_i = 1.78$ , $L/D_i = 0.39$ , $N_{GR_L} = 194,000$ , $N_{RA_L} = 137,400$ . . . . .	51
15. Photograph of Flow Pattern for $D_o/D_i = 1.78$ , $L/D_i = 0.39$ , $N_{GR_L} = 246,700$ , $N_{RA_L} = 174,600$ . . . . .	53
16. Photograph of Flow Pattern for $D_o/D_i = 1.78$ , $L/D_i = 0.39$ , $N_{GR_L} = 275,000$ , $N_{RA_L} = 194,600$ . . . . .	54
17. Periodic Interior Contraction Flow for $D_o/D_i = 1.78$ , $L/D_i = 0.39$ , $N_{GR_L} = 323,000$ , $N_{RA_L} = 228,400$ . . . . .	55
18. Sketch of Flow Pattern for $D_o/D_i = 1.40$ , $L/D_i = 0.20$ , $N_{GR_L} = 8,400$ , $N_{RA_L} = 5,950$ . . . . .	57
19. Photograph of Flow Pattern for $D_o/D_i = 1.40$ , $L/D_i = 0.20$ , $N_{GR_L} = 8,400$ , $N_{RA_L} = 5,950$ . . . . .	58
20. Steady Crescent Eddy Pattern for $D_o/D_i = 1.40$ , $L/D_i = 0.20$ $N_{GR_L} = 25,000$ , $N_{RA_L} = 17,700$ . . . . .	59
21. Photograph of Flow Pattern for $D_o/D_i = 1.40$ , $L/D_i = 0.20$ , $N_{GR_L} = 99,300$ , $N_{RA_L} = 70,000$ . . . . .	61
22. Photograph Showing Counter Rotating Cells in Upper Region of Annulus for $D_o/D_i = 1.40$ , $L/D_i = 0.20$ , $N_{GR_L} = 103,800$ , $N_{RA_L} = 73,200$ . . . . .	63
23. Photograph Showing Counter Rotating Cells in Upper Region of Annulus for $D_o/D_i = 1.40$ , $L/D_i = 0.20$ , $N_{GR_L} = 103,800$ , $N_{RA_L} = 73,200$ . . . . .	64
24. Three-Dimensional Spiral Motion in Upper Gap Region for $D_o/D_i = 1.40$ , $L/D_i = 0.20$ , $N_{GR_L} = 103,800$ , $N_{RA_L} = 73,200$ . . . . .	65

Figure	Page
25. Sketch of Steady Dog-Face Pattern for $D_o/D_i = 2.17$ , $L/D_i = 0.59$ , $N_{GR_L} = 248,800$ , $N_{RA_L} = 2,812,000$ . . . . .	67
26. Steady Dog-Face Pattern for $D_o/D_i = 2.17$ , $L/D_i = 0.59$ , $N_{GR_L} = 248,800$ , $N_{RA_L} = 2,812,000$ . . . . .	68
27. Steady Dog-Face Pattern (Upper Portion) for $D_o/D_i = 2.17$ , $L/D_i = 0.59$ , $N_{GR_L} = 248,800$ , $N_{RA_L} = 2,812,000$ . . . . .	69
28. Photograph of Flow Pattern for $D_o/D_i = 2.17$ , $L/D_i = 0.59$ , $N_{GR_L} = 1,345,000$ , $N_{RA_L} = 12,554,000$ . . . . .	71
29. Steady Dog-Face Pattern for $D_o/D_i = 1.78$ , $L/D_i = 0.39$ , $N_{GR_L} = 404,000$ , $N_{RA_L} = 3,992,000$ . . . . .	73
30. Sketch of Tertiary Flow Pattern for $D_o/D_i = 1.78$ , $L/D_i = 0.39$ , $N_{GR_L} = 1,688,000$ , $N_{RA_L} = 14,170,000$ . . . . .	75
31. Tertiary Flow Pattern (Upper Portion) for $D_o/D_i = 1.78$ , $L/D_i = 0.39$ , $N_{GR_L} = 1,688,000$ , $N_{RA_L} = 14,170,000$ . . . . .	76
32. Tertiary Flow Pattern (Upper Portion) for $D_o/D_i = 1.78$ , $L/D_i = 0.39$ , $N_{GR_L} = 1,688,000$ , $N_{RA_L} = 14,170,000$ . . . . .	77
33. Steady Dog-Face Pattern (Upper Portion) for $D_o/D_i = 1.40$ , $L/D_i = 0.20$ , $N_{GR_L} = 117,000$ , $N_{RA_L} = 1,115,000$ . . . . .	78
34. Photograph of Flow Pattern (Upper Portion) for $D_o/D_i = 1.40$ , $L/D_i = 0.20$ , $N_{GR_L} = 1,224,000$ , $N_{RA_L} = 8,322,000$ . . . . .	80
35. Three-Dimensional Spiral Motion in Upper Gap Region for $D_o/D_i = 1.40$ , $L/D_i = 0.20$ , $N_{GR_L} = 2,497,000$ , $N_{RA_L} = 14,946,000$ . . . . .	82

Figure	Page
36. Photograph of Flow Pattern (Upper Portion) for $D_o/D_i$ = 1.09, $L/D_i = 0.04$ , $N_{GR_L} = 1,840$ , $N_{RA_L} = 18,300$ . . .	84
37. Photograph of Flow Pattern (Lower Portion) for $D_o/D_i$ = 1.09, $L/D_i = 0.04$ , $N_{GR_L} = 1,840$ , $N_{RA_L} = 18,300$ . . .	85
38. Temperature Profiles for Water, $D_o/D_i = 1.40$ , $L/D_i =$ 0.20, $N_{GR_L} = 1,217,000$ , $N_{RA_L} = 7,923,000$ . . . . .	99
39. Sketch of Steady Dog-Face Pattern for $D_o/D_i = 1.40$ , $L/D_i = 0.20$ , $N_{GR_L} = 1,217,000$ , $N_{RA_L} = 7,923,000$ . . .	100

## ABSTRACT

Natural convective flow of air and water between isothermal concentric spheres was experimentally investigated. Different visualization techniques were utilized for each specified fluid. A special visualization technique was developed for water as the working medium in this study. The visualization of the flow pattern was accomplished by introducing a well mixed and prepared solution of distilled water containing a very minute amount of liquid "Ajax" detergent into the annulus and transversely illuminating vertical diameter. For air in the gap, smoke was introduced. A qualitative description of the flow patterns obtained for each spherical combination studied is presented, and these descriptions are supplemented by photographs of the flow. Motion pictures of each distinctive type of flow pattern found to occur in this investigation were also obtained.

For air as the working fluid, distinct steady and unsteady patterns were obtained for various diameter ratios ranging from 1.40 to 2.17 and for Grashof numbers (based on gap thickness) ranging from  $7.0 \times 10^3$  to  $1.2 \times 10^6$ . The flow patterns at the lower Grashof numbers qualitatively agree with those obtained in previous studies. The inception of instabilities characterized by periodic interior contractions or three-dimensional spiral flow in the spherical annuli was compared to the case of horizontal cylindrical annuli.

For water as working fluid, the most common basic flow pattern, the steady dog-face type, occurred in the three largest diameter ratios investigated. This kind of flow pattern has never been observed before, but it does correlate quite well with the temperature profiles obtained in the heat transfer study. A formation of tertiary flow in the weak shear layer between two secondary cells occurred for the diameter ratio of 1.78 ( $L/D_i=0.39$ ) at high Grashof numbers. As the Grashof number was increased above certain transition points, an unsteady dog-face type flow, or a three-dimensional spiral flow, was observed. In this study, the diameter ratio ranged from 1.09 to 2.17 and the Grashof number based on gap thickness ranged from  $1.7 \times 10^3$  to  $1.4 \times 10^7$ .

A tabular form of the experimental results for each test fluid is presented to provide categorization of the fluid-flow behavior within the available ranges of independent variables.

## NOMENCLATURE

Symbol	Description
a, b	Characteristic physical dimensions
$C_p$	Fluid specific heat at constant pressure
D	Diameter
g	Acceleration of gravity, 32.174 ft/sec <sup>2</sup>
H	Height of vertical plate
k	Fluid thermal conductivity
L	Distance between plates; gap thickness (difference between outer and inner spherical radii)
$N_D$	Characteristic physical dimension ratio
$N_{GR_a}$	Grashof number, $\rho^2 g \beta (T_i - T_o) a^3 / \mu^2$ , a is replaced by any desired characteristic dimension
$N_{PR}$	Prandtl number, $C_p \mu / k$
$N_{RA_a}$	Rayleigh number, $\rho^2 g \beta (T_i - T_o) a^3 C_p / \mu k$
r	Radial coordinate
$r_{avg}$	Average radius, $r_{avg} = (r_i + r_o) / 2$
T	Temperature
$\Delta T$	Temperature difference between inner and outer spheres, $T_i - T_o$
$\alpha$	Thermal Diffusivity, $k / \rho C_p$
$\beta$	Thermal expansion coefficient
$\phi$	Angular coordinate measured from upward vertical axis

Symbol	Description
$\mu$	Dynamic viscosity of the fluid
$\rho$	Fluid density

Subscripts

am	Arithmetic mean
i	Refers to inner sphere
L	Based on distance between plates or gap thickness
o	Refers to outer sphere
vm	Volume weighted mean

## CHAPTER I

### INTRODUCTION

In recent years, a considerable amount of interest has developed in the subject of natural convection from a body to its finite enclosure. This particular heat transfer and fluid mechanics problem is becoming increasingly important in certain areas such as nuclear design, aircraft cabin design, and electronic instrumentation packaging. However, only relatively little information has been reported in this area.

Since 1964, an important beginning in this broad area has been made in the study of natural convection between concentric isothermal spheres. The first investigation, using air as the gap fluid, was carried out by Bishop, Kolflat, Mack, and Scanlan [1]. Utilizing the techniques reported in [2], they described the flow patterns observed visually and photographically. Heat transfer data, temperature distributions, and additional comments on the flow patterns were presented by Bishop et al [3]. An analytical prediction of both thermal and flow fields by Mack and Hardee [4] is valid only for low Rayleigh numbers. The most recent studies are those of Scanlan, Bishop, and Powe [5], and Weber, Powe, Bishop, and Scanlan [6]. They extended the existing heat transfer data and temperature distributions of Bishop et al [3] ( $N_{PR} \sim 0.7$ ) to include Prandtl numbers up to 4184 by using water and two silicone fluids as

working media for both concentric and vertically eccentric cases.

Unfortunately, most of these previous studies are restricted to the heat transfer rates and temperature fields; there is little information available concerning the flow field of this specific geometrical configuration. In order to fully understand the convection process, both thermal and flow phenomena must be known. Therefore, the purpose of the current investigation is to attempt to alleviate the problem of the serious lack of knowledge of the flow behavior in this particular geometry. The attempts made in this current study are to extend the existing data of Bishop et al [1] to a higher impressed temperature difference with air as the working fluid and to establish further study of this configuration with water as the gap fluid.

The flow process resulting from the density change caused by a temperature gradient within the gravitational force field between concentric isothermal spheres can be represented by a mathematical model which includes a set of simultaneous, non-linear, coupled, partial differential equations subject to the associated boundary conditions. The analytic treatment of this problem is very difficult. This is due to the following reasons: (1) the non-linearity of the governing equations, (2) the invalidity of the general boundary layer approximations in this case, and (3) the lack of information of boundary conditions, especially when the flow field is not steady and

therefore not necessarily symmetrical about a vertical axis through the center of the spheres. These equations are shown in Appendix I.

The purposes of the present experimental investigation concerning the flow phenomena between concentric isothermal spheres are:

- (1) To obtain criteria for predicting the fluid-flow behavior within the gap as the radial distance and the temperature difference between spheres are varied. Both air and water are used as the enclosed fluids. These criteria will allow prediction of the type of flow which will occur under a variety of conditions.
- (2) To study the mechanism which determines when and how the onset of instability in the flow field occurs.

Furthermore, the results of this present work should contribute to a greater understanding of the natural convection process between isothermal spheres by correlating these with the existing data concerning heat transfer rates and temperature profiles. Also, the information described in this dissertation may be used as a guide to validate future analytical and numerical studies of natural convective flows in this spherical geometry.

## CHAPTER II

### LITERATURE REVIEW

Natural convection from a surface to its infinite surroundings has been studied by a number of investigators, and a rather large number of papers are available in the literature on this subject. The more recent contributions have been made relative to natural convection within enclosed spaces. However, there is still only a limited amount of information available concerning natural convective flow phenomena within confined spaces.

Good reviews of the early work concerned with the natural convection process can be found in several textbooks such as Jakob [7], Eckert and Drake [8], and Gröber, Erk, and Grigull [9]. Two things are generally agreed upon in the literature on natural convection. One is that the natural convection process is dominated by both fluid-flow and heat transfer considerations. Second is that the natural convection process within confined spaces, defined by two characteristic dimensions, can be characterized by the following dimensionless parameters:

$$N_{GR_a} = \frac{\rho^2 g \beta \Delta T a^3}{\mu^2} \quad (2-1)$$

$$N_{PR} = \frac{C_p \mu}{k} \quad (2-2)$$

and  $N_D = \frac{a}{b} \quad (2-3)$

(Actually there are two more parameters,  $\frac{g\beta a}{C_p}$  and  $\beta\Delta T$ , but these usually are not needed.) In these equations "a" and "b" are characteristic dimensions,  $\Delta T$  is a suitably defined temperature difference,  $N_{GR_a}$  is the Grashof number based on dimension "a",  $N_{PR}$  is the Prandtl number, and  $N_D$  is a dimensionless ratio of the characteristic dimensions. All the fluid properties are normally evaluated at either an arithmetic mean temperature or a volume-weighted mean temperature. An additional dimensionless group, the Rayleigh number ( $N_{RA_a}$ ), has been found convenient in certain cases to replace the Grashof number. The Rayleigh number is the product of the Prandtl and Grashof numbers:

$$N_{RA_a} = N_{PR} \cdot N_{GR_a} = \frac{\rho g \beta \Delta T a^3}{\alpha \mu} \quad (2-4)$$

In the present review, specific attention is directed toward natural convective flows between a body and its finite enclosure. For the case with small gap thickness and large radius of curvature, the spherical geometry can be approximated by a plane wall enclosure. Therefore a short review of the literature in this area is also presented for completeness. For clarity, the discussion is presented in three separated parts based on different geometrical configurations. These are (1) parallel plates and rectangular enclosures, (2) concentric cylindrical annuli, and (3) spherical annuli.

## PARALLEL PLATES AND RECTANGULAR ENCLOSURES

Usually no convective motion occurs in a fluid which is enclosed between two parallel horizontal plates with the upper plate maintained at a higher temperature than the lower. In a normal fluid for which the density decreases with temperature, such a temperature field will yield a stable situation in which the less dense layers are located above the denser fluid. Heat is transferred from the upper plate to the lower plate by conduction, and a linear temperature distribution is expected. However, when the lower plate is at the higher temperature, resulting in the less dense layer at the bottom, an unstable situation will be produced. Nevertheless, there is no convective flow before the critical Rayleigh number of 1,705 (based on the gap thickness) is reached. Upon exceeding this value the flow field will be a cellular structure with more or less regular hexagonal cells, in which the flow moves upward in the center and returns downward near the sides or vice versa depending upon the properties of the fluid. This flow situation is maintained up to a Rayleigh number of around 45,000. Above this value of Rayleigh number the flow changes to irregular turbulent. Chandra [10] found that the value of the critical Rayleigh number changes depending upon the layer thickness. It was reported by Schmidt and Saunders [11] that the length of the horizontal side of a cell was twice the layer depth. The more recent

work is that of Leontiev and Kirdyashkin [12]. They did an experimental study of flow patterns and temperature fields with 96% ethyl alcohol as the test liquid. To visualize the flow, well-wettable aluminum particles 5-20 microns in size were placed in the alcohol. They reported that polygonal structure of the flow in a horizontal layer was observed for Rayleigh numbers  $N_{RA_L} < 95,000$ . The flow in a polygonal cell is laminar with a motion of radial flow from the bounding sides of the polygon to the center. At  $N_{RA_L} \sim 10^5$ , the polygonal structure of the liquid flow ceases completely and transforms into a roller structure.

Natural convection across a closed cavity between vertical boundaries at different temperatures was studied by Batchelor [13]. He investigated this problem in three cases; (1) small Rayleigh numbers ( $N_{RA_L} < 10^3$ ) with  $H/L$  (ratio of cavity height to width) approximately unity, (2) general Rayleigh numbers with large  $H/L$ 's, (3) large Rayleigh numbers with general  $H/L$ 's. An analytical solution for the first case was found by utilizing a method of expanding the stream function and temperature in power series in terms of the Rayleigh number. He also obtained the solution for the last two cases by making drastic idealizations. He predicted transition to turbulent flow at  $N_{RA_L} = 13,700$  for air in the second case, and at  $N_{GR_L} = 10^9 (H/L)^{-3}$  for air (perhaps for other fluids also) in the last

case.

Using the same configuration, both experimental and numerical investigations were performed by Elder [14, 15]. The flow was made visible in his experimental study by using aluminum powder suspended in the fluid. The velocity measurements were made either by direct observation or from time photographs, in which the streak-length is proportional to the velocity. A steady secondary flow was observed in the interior region of the flow for  $N_{RA_L} \sim 10^5$ . Further, it was found that the secondary flows, when of sufficient amplitude, were able to generate other steady flows, called tertiary flows. Both photographs and sketches of the flow patterns were presented for various gap widths and Rayleigh numbers. In addition, the velocity profiles were also plotted for the half height along the gap at various Rayleigh numbers. His numerical solution was checked with the thermal and flow field data of Eckert and Carlson [16], and this comparison did show that both results are comparable.

Wilkes and Churchill [17] applied numerical techniques to a long rectangular channel with air as the enclosed fluid. The streamlines were obtained for Grashof numbers up to  $10^5$  and for various height-to-width ratios.

## CONCENTRIC CYLINDRICAL ANNULI

Another geometry which appears to yield flow results applicable to the study of concentric spheres is concentric cylindrical annuli. Several investigations using this configuration in natural convection have been carried out experimentally, analytically, and numerically. These studies cover a wide range of diameter ratios, Grashof numbers, and various gap fluids.

Liu, Mueller, and Landis [18] carried out an experimental study utilizing air, water, and Dow silicone fluid No. 200 as the working media. Five sets of concentric tubes, having diameter ratios ( $D_o/D_i$ ) ranging from 1.154 to 7.500, were used in their study. Different observation techniques were used for various working fluids in the gap. For air, tobacco smoke was introduced into the gap; in water, a blue-dye-water mixture was slowly injected under isothermal conditions. A small quantity of neutrally buoyant polyethylene particles added to the silicone fluid permitted visual and photographic observations. General descriptions and sketches of the flow patterns which were observed were presented.

A numerical solution to the problem of natural convective flow, with air as the medium, in cylindrical annuli was also reported in the form of plots of the stream function for the range of  $2 \leq D_o/D_i \leq 57$  and  $1 \leq N_{GR_{D_i}} \leq 10^5$  by Crawford and Lemlich [19]. Their results

are in accordance with the appropriate qualitative flow patterns obtained experimentally by Liu et al [18] at a diameter ratio  $D_o/D_i = 2.0$ .

Grigull and Hauf [20] presented numerous photographs, taken by introducing smoke to make the flow visible in a normal incident light plane, and sketches of flows. The annulus was filled with air at atmospheric pressure. Various gap width-to-inner diameter ratios ( $0.15 \leq L/D_i \leq 2.65$ ) were selected in their study. Three different types of convective flow phenomena as the Grashof number was changed were postulated. These are (1) a two dimensional pseudo-conductive regime for  $N_{GR_L} < 24,000$ , (2) a regime of transition with a three dimensional convective motion for  $24,000 \leq N_{GR_L} \leq 30,000$ , and (3) a regime of fully developed two dimensional laminar convective motion for  $30,000 \leq N_{GR_L} \leq 716,000$ .

An experimental investigation of the flow behavior for natural convection in simple and obstructed horizontal cylindrical annuli was performed by Lis [21] using the Schlieren technique. A few photographs and verbal descriptions of the flow patterns were presented in his report for various diameter ratios and Grashof numbers.

Bishop and Carley [22] carried out a photographic experimental study of natural convective flows of air between concentric horizontal cylinders. Photographs and qualitative descriptions of

the flow patterns were obtained for various operating conditions at diameter ratios ranging from 1.23 to 3.69, with temperature differences of 5°F to 100°F between the cylinders. They found two types of stable flow and one unstable flow within their range of diameter ratios. Under all temperature differences studied for diameter ratios of 1.23, 1.85, and 2.46, the first stable flow, termed a "crescent eddy" type, existed at low Grashof numbers. Another stable flow pattern, the "kidney-shaped eddy" type, was found to appear for a diameter ratio 3.69 at Grashof numbers above that at which the crescent eddy flow pattern disappeared. For higher Grashof numbers, this pattern became an unstable oscillation of the fluid in the upper region of the gap. They also found that both frequency and amplitude of oscillation were increased at increasing temperature difference.

Employing the technique set forth by Batchelor [13] to expand the stream function and temperature in an infinite series of Rayleigh number, an analytic solution, limited to low values of Rayleigh number, was reported by Mack and Bishop [23]. They found that increasing the Prandtl number above 0.70 had very little effect upon the qualitative appearance of the stream lines at low Rayleigh number, except for very small Prandtl number fluids such as liquid metals.

An extensive study of the three dimensional oscillatory flow in cylindrical annuli, observed by Bishop and Carley [22], was carried

out by Bishop, Carley, and Powe [24]. Correlation equations were given to allow estimation of the inception of this oscillatory flow and its subsequent amplitude, period, and wave length. Detailed descriptions of this particular flow phenomenon supported by photography and motion pictures also can be found in Powe [27].

Bishop and Carley [22] compared their results with these of Liu et al [18] and pointed out the very interesting possibility of obtaining different types of flows for a given diameter ratio while using different cylinder sizes. Powe [27] investigated this possibility experimentally for air within the gap as reported by Powe, Carley, and Bishop [25]. Using six different cylinder sets, two of them yielding the same diameter ratio with different cylinder sizes, and varying both the annulus pressure and temperature difference between the cylinder surfaces, they observed one steady and three unsteady flow patterns in the range of Grashof number (based on annulus width) from 300 to  $3.4 \times 10^6$ . They pointed out that radius of curvature, though not affecting the general type of the flow pattern, did affect the specific value of Grashof number at which transition from a steady to an unsteady pattern occurred. A plot categorizing the flow patterns in horizontal concentric cylindrical annuli filled with air was presented showing the transition Grashof number versus ratio of inner-cylinder diameter-to-annulus width by combining their data and several existing previous

experimental results.

The results of a numerical investigation, utilizing finite-difference techniques, to this problem were presented by Powe, Carley, and Carruth [26]. The results were compared with the existing data and excellent agreement was found. This numerical solution can also be used to predict the Rayleigh numbers where the flow will go from a stable condition to an unstable condition for a wide range of inverse relative gap widths ( $D_i/L$ ) from 2.8 to 12.5. This is due to the occurrence of steady secondary flows immediately preceding the unsteady flow, which has been observed in experimental investigations within the above specified inverse relative gap widths. It was found that a pronounced increase in magnitude of temperature and velocity components heralded the appearance of secondary flow in the large inverse relative gap widths.

#### SPHERICAL ANNULI

An initial investigation of the natural convection process in the annulus between concentric spheres was carried out by Bishop, Scanlan, and their colleagues in 1964. Since that time a series of papers have been published.

The first investigation was carried out by Bishop, Kolflat, Mack, and Scanlan [1] for air as the working medium within the gap. Using

the flow visualization techniques described in [2], they observed three different flow behaviors for diameter ratios of 1.19, 1.72, and 3.14 at various temperature differences ( $5^{\circ}\text{F} \leq \Delta T \leq 60^{\circ}\text{F}$ ). The most common pattern, the crescent-eddy type, occurred for the intermediate diameter ratio (1.72) at all temperature differences, while for the largest (3.14) and the smallest (1.19) diameter ratios it occurred only at small temperature differences. The second flow pattern, the kidney-shaped eddy type, occurred for the largest diameter ratio (3.14), i.e., the largest gap, at moderate to large temperature differences. The main difference between the first two patterns was the shape of the central-eddy region. The third flow pattern, the "falling-vortices" type, occurred at moderate to high temperature differences for the smallest diameter ratio (1.19). This flow type was unsteady and was characterized by the formation and shedding of vortex cells. Detailed descriptions and photographs concerning these three different flow patterns were also presented. Further details of this study were given by Bishop [28]. The results of an investigation of heat transfer rates and a detailed discussion of temperature distributions correlated to the observed flow patterns were presented by Bishop et al [3].

An analytical solution to this problem was carried out by Mack and Hardee [4] in the same manner as that of Mack and Bishop [23] for concentric cylinders. This solution is limited to low values of

Rayleigh number. Their highest value of Rayleigh number was considerably below the lowest value obtained experimentally by Bishop et al [3].

The two most recent reports were contributed by Scanlan, Bishop, and Powe [5] and Weber, Powe, Bishop, and Scanlan [6]. Scanlan et al [5] extended the existing heat transfer data and temperature profiles of Bishop et al [3] ( $N_{PR} \sim 0.70$ ) to include Prandtl numbers up to 4184 by introducing water and two different silicone fluids into the gap. The first investigation concerning natural convection between eccentric spheres was performed by Weber et al [6]. They introduced a conformal mapping technique to present the results of heat transfer rates between eccentric spheres to enable a comparison with the existing data for concentric spheres. A single correlation equation of heat transfer rates was obtained for an extremely wide range of diameter ratios, eccentricities, Rayleigh numbers, and Prandtl numbers. They also pointed out that the effect of a negative eccentricity (inner sphere below the center of the outer sphere) on the temperature distribution was basically an enhancement of the convective motion, while a positive eccentricity tended to stabilize the flow field and promote conduction rather than convection. The multicellular flow pattern, which has previously been postulated by Bishop et al [3] to explain the temperature distribution between concentric spheres with small gap spacing, was

also found to yield a plausible explanation for the thermal field obtained using the largest inner sphere ( $D_i = 9''$ ) considered in their investigation.

In addition, natural convection heat transfer between isothermal centrally located vertical cylinders and their isothermal spherical enclosure was experimentally investigated by Weber [29]. Various diameters of cylinders and aspect ratios, defined as the ratio of length of straight cylindrical section to radius of cylinder, were used in his study with the gap filled with water. Based upon his measured heat transfer rates and temperature distributions, he noted that the larger aspect ratios for all diameter ratios seemed to curtail the convective activity while the smaller aspect ratios for all diameter ratios seemed to promote convective activity. A multicellular flow regime was also postulated for the smallest diameter ratio cylinder investigated.

## CHAPTER III

### EXPERIMENTAL APPARATUS AND PROCEDURE

#### EXPERIMENTAL APPARATUS

The apparatus used in this investigation was designed to provide the capability to study the characteristics of natural convective flow between isothermal concentric spheres with different diameter ratios using both air and water as the gap media. A photograph of the assembled apparatus, utilizing water as the gap fluid, is shown in Figure 1. Figure 2 and Figure 3 present schematics of the entire operating system for water and air as the gap working fluid respectively. An equipment list is provided in Appendix II for reference purposes.

The same inner spheres, 9.00, 7.00, 5.50 and 4.50 inches in diameter, used in the heat transfer study by Scanlan et al [5] were also used in the current study. All of the inner spheres were fabricated from copper with an approximate wall thickness of 0.025 inch. In order to establish the flow visualization, a glass outer sphere was fabricated from two hemispheres with an inner diameter of 9.77 inches. The combination yielded diameter ratios ( $D_o/D_i$ ) of 1.09, 1.40, 1.78, and 2.17 which are close to the values used in the heat transfer study of Scanlan et al [5]. This arrangement will allow convenient correlation between thermal and flow phenomena for this geometry.

The inner spheres were supported in the outer sphere by a































































































































































































































